Effects of Local Electric Field and Effective Tunnel Mass on the Simulation of Band-to-Band Tunnel Diode Model

Kyung Rok Kim and Robert W. Dutton
CISX 302, Stanford University, Stanford, CA 94305, USA
Phone: (650) 725-6240, Fax: (650) 725-7731, Email: krkim@gloworm.stanford.edu

Abstract **– We propose a numerical band-to-band tunneling model that is suitable for forward-biased silicon tunnel diode simulation. In this model, the tunneling attenuation factor, which depends on the local electric field and effective tunnel mass, determines the tunneling rate and negative differential resistance characteristics of the tunnel diode. Simulation results with the reduced tunnel mass m_{rx}*= 0.10m_o considering conductivity electron mass in the conduction band and light-hole mass in the valence band show good agreement with the theoretical calculations for reasonable doping ranges ($2.5k_BT < qV_{n,p} < 7.5k_BT$). This local BTBT model is advantageous for fast simulation of tunnel devices using numerical device simulators.**

I. Introduction

In recent researches, band-to-band tunneling (BTBT) in silicon (Si) has received much attention as nanoscale CMOS devices with narrow drain-to-channel junctions have increased leakage [1]. Some devices exploit this tunneling current as an active operation current to be increased [2]. Research regarding the enhancement of CMOS performance has focused on reverse-biased BTBT from the valence band to conduction band. For this reason, BTBT models in numerical device simulators are only available for the case of reverse-biased junctions [3, 4] and they cannot calculate forward tunneling current in the simulation of tunnel diode structures with degenerate junction (Fig. 1(a)).

However, forward BTBT transport from the conduction band to valence band is also attractive since it provides a portion of negative differential resistance (NDR), which has versatile functionality with minimal device complexity. The pioneering work of Esaki in 1958 [5] initiated intensive experimental and theoretical investigations; various functional NDR devices using forward BTBT characteristics have been implemented with 2-terminal diode [6] or 3-terminal transistor structures based on Si CMOS technologies [7, 8]. These Si NDR devices should coexist with CMOS transistors for better performance in digital and analog circuit applications. Therefore, for the efficient simulation of these functional NDR devices, a numerical forward BTBT model should be implemented in TCAD-based device simulators.

Since BTBT effects can basically be considered as the generation or recombination of electron-hole pairs, the existing reverse BTBT model has been incorporated into the generation-recombination (GR) term in the electron and hole continuity equation. In this paper, we present a local GR model for the calculation of forward BTBT transport from conduction band to valence band. In the following sections, we discuss the model based on locality and investigate effects of local electric field and effective tunnel mass on the simulation of Si BTBT diode in a numerical device simulator.

II. Tunnel Diode Structure

Figure 1 (a) shows the band diagram of a Si tunnel diode at thermal equilibrium with $N_a = N_d = 5 \times 10^{20}/cm^3$. When the doping concentration is above the effective density of states in the conduction band ($N_C = 2.8 \times 10^{19}/cm^3$) and valence band ($N_V = 1.05 \times 10^{19}/cm^3$), the Fermi level ($E_{fn}$, E_{fp}) is located within the allowed bands. The dependencies of degeneracy ($\eta_n = (E_{fn} - E_c)/k_BT$, $\eta_p = (E_v - E_{fp})/k_BT$) on doping concentrations are summarized in Fig. 1 (b) based on Fermi-Dirac and Boltzmann statistics, respectively. Considering the thermal energy and solid solubility, we take a reasonable doping concentration range from $1 \times 10^{20}/cm^3$ to $5 \times 10^{20}/cm^3$ ($2.5k_BT < qV_{n,p} < 7.5k_BT$) for the following tunnel diode simulations.

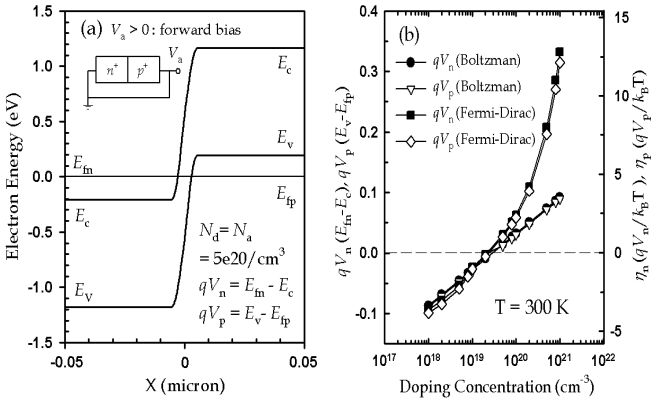

Fig. 1. (a) Energy band diagram of Si tunnel diode at thermal equilibrium. Doping concentrations are as $N_d = N_a = 5 \times 10^{20}/cm^3$. (b) Degeneracy ($\eta_n$, η_p) dependencies on the doping concentration based on the Boltzman and Fermi-Dirac statistics, respectively

III. BAND-TO-BAND TUNNELING MODEL

For the numerical simulation of forward-biased BTBT current and NDR characteristics in the tunnel diode structure, a local GR model of the BTBT effect, which is suitable for implementation in TCAD-based numerical device simulators, is proposed as follows:

$$R_{BB} = -A \cdot D_E \cdot F^2 \cdot \exp\left(-F_o/F\right) \tag{1}$$

where A is a constant, D_E is a net-rate factor, F is local electric field, and F_o is the characteristic electric field, which contains the effective tunnel mass dependence. This basically extends the Hurkx BTBT recombination model [4], which is valid in zero and reverse bias, to the forward bias region. In a strict sense, D_E should be described non-locally with the relative positions of the Fermi levels E_{fn} and E_{fp} in the neutral regions. In this local model, however, D_E can be represented by local intrinsic ($\psi = -E_i(x)/q$) and quasi-Fermi level ($\phi_n(x) = -E_{fn}(x)/q$ and $\phi_p(x) = -E_{fp}(x)/q$) as

$$D_E = \frac{1}{\exp\left[\left(E_i(x) - E_{fn}(x)\right)/k_B T\right]+1} - \frac{1}{\exp\left[\left(E_i(x) - E_{fp}(x)\right)/k_B T\right]+1} \tag{2}$$

since the locality is practically valid near equilibrium and in the forward bias region where the tunneling current density is not so high, the generated electron and hole densities are lower than the intrinsic carrier density. Figure 2 shows the net rate factor (left y-axis) at the middle of the gap (x = 0) as a function of applied voltage V_a. By applying this local factor D_E in the forward bias case, the generation of electron-hole pairs by BTBT from the conduction band to valence band can be modeled.

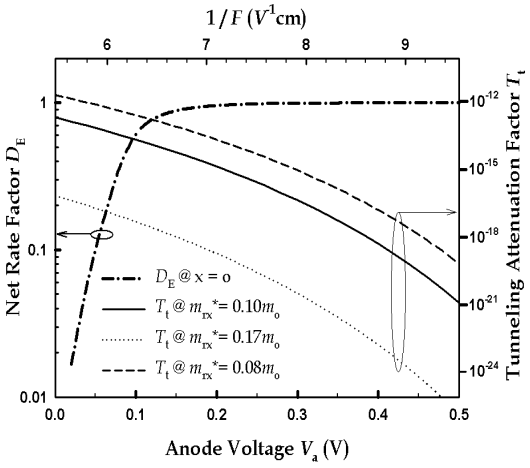

Fig. 2. Plot of the net-rate factor D_E (left y-axis) and the tunneling attenuation factor T_t (right y-axis) as a function of applied bias and corresponding electric field in the middle of the tunnel junction.

In the case of indirect band-gap material such as Si, the forward NDR characteristics result from the tunneling attenuation factor based on electric field rather than non-local density of states in the neutral region. Namely, they have a stronger field dependence than direct band-gap material because of the extra "perpendicular" degrees of freedom [9]. Therefore, in this local GR model (eq. (1)), the tunneling attenuation factor ($T_t = exp\ (-F_o/F)$) should have a dominant effect in the determining the NDR shape. Figure 2 shows that increasing forward bias ($V_a > 0$) from 0 to 0.5 V causes a dramatic decrease of the tunneling attenuation factor (right y-axis) by nine orders of magnitude at the effective tunnel mass ratio (m^*_{rx}/m_o) of 0.1 in F_o. The characteristic electric field F_o in this model is determined based on the WKB approximation as

$$F_o = b \cdot \frac{(E_g - \hbar\omega_{TA})^{3/2}}{q\hbar} \cdot \sqrt{2m_{rx}^*} \tag{3}$$

where b is a constant related with barrier shape, E_g is a band-gap energy, $\hbar\omega_{TA}$ is the acoustic phonon energy in phonon-assisted indirect tunneling, and m^*_{rx} is the reduced tunnel mass, which contains the physical information such as band structure and tunneling direction.

In the Si tunnel diode, we assume that BTBT takes place between the light-hole band for holes and the conduction band minima for electrons. Thus, we assume the reduced tunnel mass considering conductivity electron mass in the conduction band [10] and light-hole mass (m_{lh}^*) in the valence band as

$$\frac{1}{m_{rx}^*} = \frac{1}{m_{lh}^*} + \frac{1}{3}\left(\frac{1}{m_L^*} + \frac{2}{m_T^*}\right) = \frac{1}{0.1m_o} \tag{4}$$

where $m_{lh}^* = 0.16m_o$, $m_L^* = 0.98m_o$ and $m_T^* = 0.19m_o$ are the longitudinal and transverse masses of electron at the conduction band minima, respectively. To investigate the influence of the effective tunnel mass on the BTBT generation rate, another two extreme values of $m_{rx}^* = 0.17m_o$ with heavy-hole mass instead of light-hole mass and $m_{rx}^* = 0.08m_o$ incorporating both heavy and light-hole into tunneling process are considered. As shown in Fig. 2, the variation of T_t is very sensitive to the effective tunnel mass ratio (m^*_{rx}/m_o). For example, using heavy-hole mass instead of light-hole mass ($m_{rx}^* = 0.17m_o$) would decrease the tunneling probability by four orders of magnitude at 1.5 x 10^6 V/cm.

Figure 3 shows the energy band diagram and the calculated BTBT generation rate at $V_a = 0.12$ V and $m_{rx}^* = 0.1m_o$. As a result of our GR model (eq. (1)), the generation rate of BTBT from conduction band to valence band has been calculated in the forward bias region ($V_a > 0$)

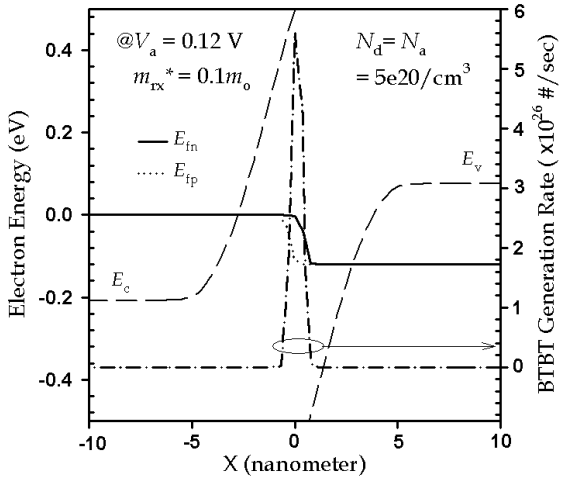

Fig. 3 Energy band diagram and the calculated BTBT generation rate at V_a= 0.12 V and m_{rx}^*= 0.1m_o in case of N_d= N_a= 5x 10^{20} /cm^3.

IV. Simulation Results and Discussion

For the numerical *I–V* simulations of the Si tunnel diode, we incorporated the proposed local BTBT model (eq. (1)) into the recombination term in the electron and hole continuity equations using Taurus-PMEI (physical model and equation interface) [11]. Figure 4 shows the simulation results of the BTBT current and NDR in the forward bias region at room temperature (T= 300 K), which indicates that the peak voltage and peak current increase as doping concentration increases. These are the first reported simulation results of forward BTBT current and NDR characteristics of the well-known "*Esaki*" diode using TCAD-based numerical device simulator based on locality.

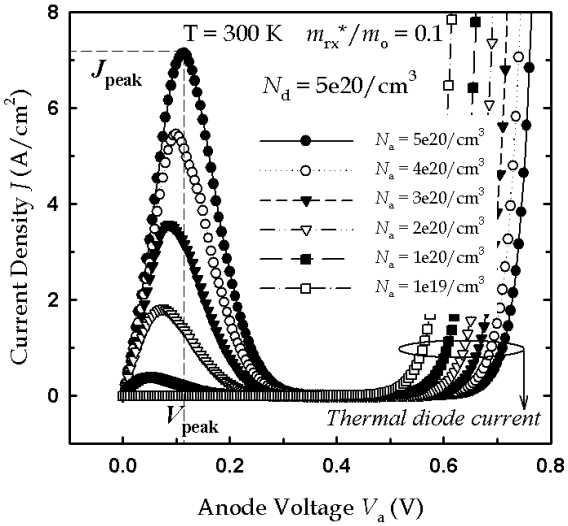

Fig. 4. Simulation results of proposed BTBT diode model for various doping conditions. The important device parameters of the peak current J_{peak} and voltage V_{peak} are noted. The effective tunnel mass ratio is fixed at m_{rx}*/m_o = 0.1.

In addition, when the doping concentrations are under 5x10^{19}/cm^3, which means the non-degenerate system, the forward BTBT current become disappeared even though the proposed GR model (eq. (1)) is included (Fig. 5). Therefore, we confirm that the model is valid both for degenerate and non-degenerate systems.

To confirm the validity of the local model, we should compare the typical parameters in tunnel diode characteristics such as peak voltage (V_{peak}) and peak current density (J_{peak}) with the theoretical calculations. Figure 6 (a) shows the normalized peak voltages as symbols extracted from the Taurus-PMEI simulations as a function of the normalized degeneracy α ($=\eta_{min}/\eta_{max}$) with m_{rx}^*= 0.08m_o, 0.10m_o, and 0.17m_o, respectively. As shown by Kane's tunneling theory [9], the values calculated from the indirect (solid line) and direct (dashed line) BTBT are also indicated. The extracted peak voltages (symbols) from the simulation with m_{rx}^*= 0.1m_o considering light-hole mass and conductivity electron mass show good agreement with the theoretical calculations from the indirect BTBT case over a wide range of the degenerate doping conditions (α). In Kane's theoretical investigations, the peak voltages from indirect BTBT case are always smaller than those from direct BTBT case that are equal to the values calculated only considering non-local density of states through finding the electron energy which produces the maximum carrier densities on each side [12]. Hence, in the case of the indirect tunneling, the bias and field dependence of NDR is more important compared to the non-local density of states in the neutral region; the proposed local BTBT model is physically valid in the forward-biased tunnel diode simulation with indirect BTBT.

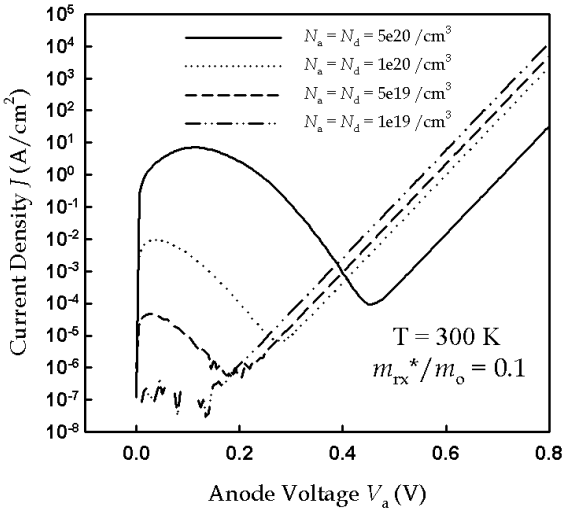

Fig. 5 Doping dependencies of BTBT current density at T= 300 K and m_{rx}*/m_o = 0.1. For doping condition below 5x10^{19}/cm^3, there is no significant BTBT current even though BTBT generation model is included.

The peak tunneling current J_{peak} is a crucial parameter for tunnel diodes in terms of the switching speed index J_{peak}/C where C is the junction capacitance. Basically, J_{peak} is enhanced as doping concentration increases; simple BTBT theory indicates that a plot of *log* J_{peak} as a function of the effective doping concentration $N_{eff} = (N_a^{-1} + N_d^{-1})^{1/2}$ should be linear [12, 13]. By plotting J_{peak} extracted from our simulation results in this way, we observe good linearity for all doping ranges ($1 \times 10^{20}/cm^3 < N_a, N_d < 5 \times 10^{20}/cm^3$).

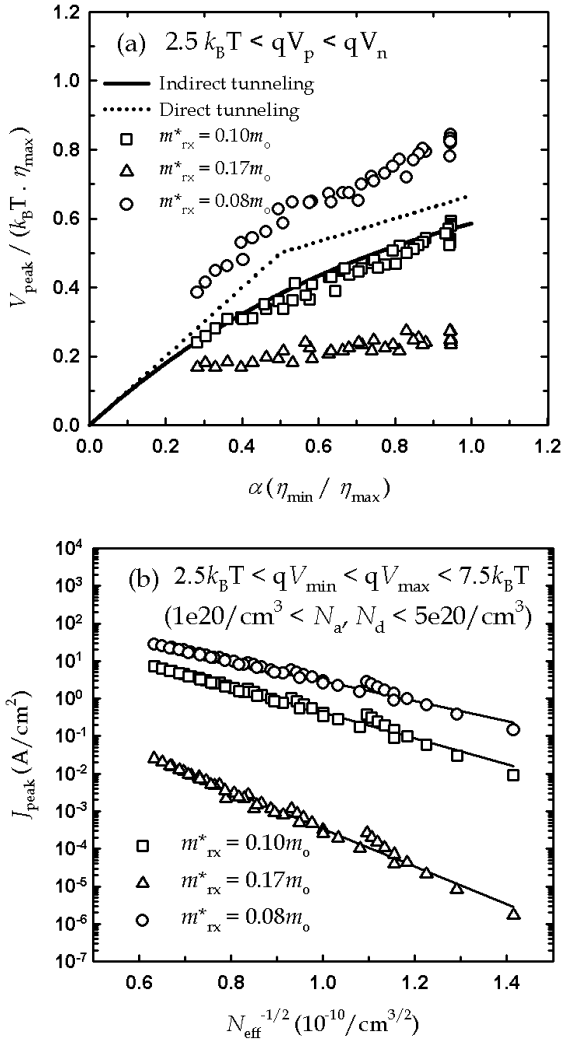

Fig. 6 (a) Normalized peak voltage as symbols extracted from the Taurus-PMEI simulations as a function of the normalized degeneracy α ($=\eta_{min}/\eta_{max}$) for three values of the reduced tunnel mass: $m_{rx}^* = 0.08m_o$, $0.10m_o$, and $0.17m_o$, respectively. (b) Plot of *log* J_{peak} extracted from our PMEI simulation results as a function of the effective doping concentration $N_{eff} = (N_a^{-1} + N_d^{-1})^{1/2}$ for $m_{rx}^* = 0.08m_o$, $0.10m_o$, and $0.17m_o$, respectively

V. SUMMARY

A local BTBT model for forward-biased tunnel junctions has been demonstrated. The effects of the tunneling attenuation factor on the simulation of forward-biased tunnel diodes have been investigated; the range of doping and effective tunnel mass conditions over which the model is applicable has been studied. This local BTBT model, which is suitable for TCAD device simulators, makes it possible to simulate various device structures with BTBT junctions on commercial TCAD platforms.

ACKNOWLEDGEMENTS

The authors would like to thank Klas Lilja of Robust Chip Inc. and Yang Liu of the Stanford TCAD group for helpful discussions and a number of useful comments. This work was supported by the Post-doctoral Fellowship Program of Korea Research Foundation (KRF) and in part through the MARCO MSD center.

REFERENCES

[1] C.-H. Choi, S.-H. Yang, G. Pollack, S. Ekbote, PR Chidambaram, S. Johnson, C. Machala, and R. W. Dutton, *Proc. of SISPAD*, 2003, p. 133.

[2] Th. Nirschl, P.-F. Wang, C. Weber, J. Sedlmeir, R. Heinrich, R. Kakoschke, K. Schrufer, J. Holz, C. Pacha, T. Schulz, M. Ostermayr, A. Olbrich, G. Georgakos, E. Ruderer, W. Hansch, and D. Schmitt-Landsiedel, *IEDM Tech. Dig.*, 2004, p. 195

[3] E. O. Kane, *J. Phys. Chem. Solids*, **12** 181 (1959)

[4] G. A. M. Hurkx , D. B. M. Klaassen, and M. P. G. Knuvers, *IEEE Trans. Electron Devices*, **39** 331 (1992)

[5] L. Esaki, *Phys. Rev.*, **109** 603 (1958)

[6] M. W. Dashiell, R. T. Troeger, S. L. Rommel, T. N. Adam, P. R. Berger, C. Guedj, J. Kolodzey, A. C. Seabaugh, and R. Lake, *IEEE Trans. Electron Devices*, **47** 1707 (2000)

[7] K. R. Kim, D. H. Kim, S.-K. Sung, J .D. Lee, and B.-G. Park, *IEEE Electron Device Letters*, **23** 612 (2002)

[8] K. R. Kim, H. H. Kim, K.-W. Song, J. I. Huh, J. D. Lee and B.-G. Park, *IEEE Trans. Nanotechnology*, **4** 317 (2005)

[9] E. O. Kane, *J. Appl. Phys.*, **32** 83 (1961)

[10] R. A. Smith, *Semiconductors*, *2nd Ed.*, Cambridge University Press, London, 1979.

[11] Taurus-Device^{TM}, *User Guide*, Synopsis Inc., Sep. 2004.

[12] T. A. Demassa and D. P. Knott, *Solid State Electron.*, **13** 131 (1970)

[13] Y. Furukawa, *J. Phys. Soc. Japan*, **15** 1903 (1960)